New Sensitive and Selective Fluorescent Probes for Fluoride Using Boronic Acids

Nicolas DiCesare, **Joseph R. Lakowicz**[1]

Center for Fluorescence Spectroscopy, University of Maryland, School of Medicine, 725 W. Lombard Street, Baltimore, Maryland 21201

Abstract

We report the spectroscopic characterization of six fluorescent probes for fluoride sensing and/or monitoring. All probes are based on the ability of the boronic acid group to interact with fluoride. The probes combine electron donor and withdrawing groups and involve the excited charge transfer mechanism. The change between the neutral form of the boronic acid group [R-B(OH)$_2$], which is an electron withdrawing group, and the anionic trifluoro form $\left[\text{R-BF}_3^-\right]$, which is an electron donating group, is at the origin of the different spectral changes observed for the investigated probes. Two probes are based on the stilbene structure where the boronic group in the 4 position is coupled with a cyano group, in one case, and the dimethylamino group in the other case, both at the 4′ position. Another probe is based on the diphenyl-1,4-butadiene possessing the boronic acid group in the 4′ position and a dimethylamino group in the 4″ position. One probe is based on the diphenyloxazole structure having both the boronic acid and the dimethylamino groups in *para* positions. The two last probes reported are based on the benzalacetophenone (chalcone) structure, again coupling the boronic acid and dimethylamino groups. All probes show spectral shifts and/or intensity changes in the presence of fluoride resulting in most of the cases to a wavelength-ratiometric way for the detection and/or analysis of fluoride. Selectivity and stability constants are also presented and discussed.

Fluorescence probes are powerful tools for noninvasive monitoring and/or analysis of specific analytes in biological sample. For several decades, the development of fluorescent probes has been the main focus of many research groups (1–5). For example, these developments have found useful applications in cellular imaging using fluorescence microscopy and in clinical chemistry (6). Fluorescent chemosensors for analyte recognition can be divided into three parts: first, the chelator group for the recognition step, second, the fluorophore for the spectral properties, and third, the mechanism to induce the spectral changes following the chelation of the analyte. As a mechanism, intramolecular charge transfer (ICT)[2] in the excited state is well known to be very sensitive to slight perturbations in the molecular structure and/or in the environment surrounding the probe (7, 8). The boronic acid group [R-B(OH)$_2$] is known for its ability to interact with "hard bases" (as OH$^-$

---

[1]To whom correspondence should be addressed. Fax: (410) 706-8408. cfs@cfs.umbi.umd.edu.

[2]Abbreviations used: ICT, intramolecular charge transfer; CSTBA, 4′-cyanostilbene-4-boronic acid; DSTBA, 4′-dimethylaminostilbene-4-boronicacid;DAPB-PBA, 1-(*p*-dimethylaminophenyl)-4-(*p*-boronophenyl)-buta-1,3-diene; DAPOX-PBA, 5-(4′-dimethylaminophenyl)-2-(4″-boronophenyl)oxazole.

and F^-) and diols (9–11). The boronic acid group has been used, for a decade, to develop very promising probes for saccharides (11–14). In one of our recent papers (15), we investigated the use of the boronic acid group as an electron withdrawing group. We find that the boronic acid group acts as an electron withdrawing group in its neutral form and as an electron donating group in its anionic form $\left[\text{R-B(OH)}_3^-\right]$. We also demonstrated that the coupling of electron donor or withdrawing groups with the boronic acid group on the same chromophore leads to the formation of the ICT state. This ICT state was shown to be very sensitive to the orbital hybridization-dependent conformational change between the neutral and anionic form of the boron group and also to chelation with sugars leading to wavelength-ratiometric probes for saccharides (15–17).

The interest in fluoride sensing comes from both academic research and industrial applications. For example, fluoride metabolites in biological systems and fluoride analysis in water or toothpastes are areas where the development of new approaches for fluoride signaling could be needed. Large doses or chronic ingestion of lower doses of fluoride can result in a variety of side effects, such as acute gastric and kidney disturbances, dental and skeletal fluorosis, or even death (18, 19). Accurate determination of fluoride can be archived using sensitive and selective electrodes prepared from LaF_3 (20). Electrochemical (21, 22) and colorimetric (23, 24) determination of fluoride using the boronic acid group has also been reported. The use of fluorescent sensors for fluoride monitoring could find useful applications, especially for medical and biochemical ones. Only a few fluorescent probes can be found in the literature (25), all based on benzene and naphthalene structures and showing absorption in the deep UV (~270 nm). A wider diversity of probes is desirable to satisfy potential applications.

In this study, we present the spectral characterization of six fluorescent probes for fluoride signaling. The probes show absorption from 325 to 450 nm and emission throughout the visible wavelength from 420 to 650 nm. The probes are based on the ability of the boronic acid to interact with fluoride to form a trifluoroboronate anion $\left[\text{R-BF}_3^-\right]$. All probes use the ICT mechanism and combine the boronic acid group with electron donating (dimethylamino) or electron withdrawing (cyano) groups. Variation in the electron withdrawing property of the boron group in the absence and in the presence of fluoride induces important spectral changes. Wavelength shift and/or intensity changes are observed. We report the stability constants and the selectivity against other anions is also discussed.

MATERIALS AND METHODS

Potassium fluoride (KF), potassium chloride (KCl), and potassium bromide (KBr) were purchase from Aldrich and used without further purification. 4′-Cyanostilbene-4-boronic acid (CSTBA), 4′-dimethylaminostilbene-4-boronic acid (DSTBA), and 1-(*p*-dimethylaminophenyl)-4-(*p*-boronophenyl)-buta-1, 3-diene (DAPB-PBA) were synthesized as previously described (15, 16). The synthesis of Chalc1, 5-(4′-dimethylaminophenyl)-2-(4″-boronophenyl)oxazole (DAPOX-PBA) and Chalc2 will be described in a future publication (17).

Absorption spectra were recorded on the Cary 50 spectrophotometer from Varian. Fluorescence spectra were recorded on the Eclipse spectrofluorometer from Varian. All measurements were done in a 1-cm quartz cuvette. For all measurements, the optical densities of the solution were around 0.1. Stability constants (K_n) were obtained by fitting the titration curves using the relation (25, 26)

$$I = \frac{I_0 + I_\infty K_n [F^-]^n}{1 + K_n [F^-]^n},$$

[1]

where I_0 and I_∞ represent the initial intensity and the intensity at the plateau. K_n is the constant representing the equilibrum

$$K_n = \frac{\left[R{-}B(OH)_{3-n} F_n \right]}{\left[R{-}B(OH)_2 \right] [F^-]^n}$$

[2]

and is schematically shown in Scheme 1.

RESULTS

The fluorescent probes investigated are shown in Fig. 1. All probes display intramolecular charge transfer in the excited state (15–17). Since the cyano group is an electron withdrawing group, CSTBA shows ICT when the anionic form of the boronic acid is induced. DSTBA, DAPB-PBA, and DAPOX-PBA show ICT for the neutral form of the boronic acid group because of the presence of the electron donating N,N-dimethylamino group. All four probes directly involved the boron group in the ICT. On the other side, Chalc1 and Chalc2 show ICT involving the N,N-dimethylamino group (donor) and the carbonyl (acceptor) group. In this case, the boronic acid group, which shows delocalization with the carbonyl group but not with the N,N-dimethylamino group, is indirectly involved in the ICT. Normalized absorption spectra of the investigated probes are shown in Fig. 2 and the spectroscopic parameters are presented in Table 1.

CSTBA

Fluoride's effect on the emission spectrum of CSTBA is shown in Fig. 3A and spectroscopic parameters are reported in Table 1. In the presence of fluoride, we observed a red shift and a decrease of the intensity of the emission band. These spectral changes are exactly the same as that observed previously (15) at high pH and are interpreted by the formation of an ICT as the anionic form of the boron group is induced as shown in Scheme 1. Since the ICT depends only on the negative charge of the boron group, the effect of F^- and OH^- is the same. In the same way, since the pK_a of CSTBA is 8.2 (15); the fluoride effect at pH higher than ~9 would be negligible.

Figure 3A displays the titration curve of CSTBA against F^-. The titration curve shows the formation of a trifluoro tetrahedral boronate form (Scheme 1) where $n = 3$ (Eqs. [1] and [2]). The stability constant is reported in Table 1 (2.9×10^3 dm^9 mol^{-3}) and is smaller then those reported for phenylboronic acid and naphthylboronic acid (1.01×10^4 and 1.08×10^4 dm^9

mol^{-3}, respectively) (25). CSTBA could detect fluoride in the range of 40 to 80 mM. Figure 3B also shows that chloride and bromide have no effect on the spectroscopic parameters of CSTBA. The absence of an effect due to chloride and bromide observed for all the investigated probes described in this study is due to the high selectivity of the boronic acid group for fluoride as described in the literature (21). Dusemund *et al.* (21) reported the stability constants of a ferroceneboronic acid compound against different anions. The stability constants with chloride, bromide, and thiocyanate are negligible and stability constants against sulfate and dihydrogen phosphate are almost a hundred-fold smaller in comparison with fluoride.

DSTBA and DAPB-PBA

Figure 4 shows the effect of fluoride on the emission spectrum of DSTBA and spectroscopic parameters are reported in Table 1. In contrast to CSTBA, we observed a blue shift in the emission band in presence of fluoride. This blue shift is due to the removal of the ICT as the anionic fluoroboronate form is formed. Similar spectral changes are also observed for DAPB-PBA (Table 1). Titration curves of DSTBA and DAPB-PBA against fluoride are shown in Fig. 5. As observed for CSTBA, the titration curves show the formation of a trifluoride boronate form. The stability constants for DSTBA and DAPB-PBA are almost 10-fold smaller in comparison with CSTBA. These results are in agreement with the higher pK_a of DSTBA (9.1) and DAPB-PBA (8.9) in comparison with CSTBA (8.2), showing that the electrophilicity of the boronic group is smaller when the boron group is coupled with an electron donating group. These two probes could be effective for fluoride sensing in the range of 100 to 200 mM.

DAPOX-PBA

Figure 6A shows the effect of fluoride on the emission spectrum of DAPOX-PBA. As observed previously, a blue shift combined with an important increase of the intensity is observed in the presence of fluoride. Both effects are interpreted by the loss of the ICT property of the excited state as discussed above. Diphenyloxazole with electron donor and acceptor groups is well known to be very sensitive and shows important spectral changes following perturbation of the ICT (27). In comparison with the other probes presented in this study and in the literature, DAPOX-PBA presents very interesting characteristics for a chemosensor for fluoride. First, it shows a large stoke shift and an emission in the long wavelength. Second, it shows a very important intensity change, 14-fold (Table 1), giving a large response and, third, it displays a high fluorescence quantum yield (0.17 in the absence of fluoride and close to unity in the presence of fluoride) giving a high signal-to-noise ratio.

Figure 6B shows the titration curves against fluoride, chloride, and bromide. The stability constant against fluoride is reported in Table 1. As observed for the other compounds, no effect on the spectral properties was observed in the presence of chloride and bromide. Surprisingly, the stability constant of DAPOX-PBA is higher than those reported for the previous compounds described (CSTBA, DSTBA, and DAPB-PBA). Since DAPOX-PBA has the same couple acceptor/donor (boronic group/ dimethylamino group) as DSTBA and DAPB-PBA, we could expect to observe similar stability constants. Deeper study would be necessary to correlate the molecular structure with the stability constant of the probes.

Chalc1 and Chalc2

Chalcone derivatives are different than the other probes described previously. For these derivatives, the boronic acid group is not directly involved in the ICT. The ICT is between the dimethylamino and the carbonyl group. Since the boronic group is in resonance with the carbonyl group, we can expect that the change between the neutral and the aninionic form of the boron group modifies the electronic density on the carbonyl group and then modifies the ICT property of the excited state. The effect of fluoride on the emission spectrum of chalc2 is shown in Fig. 7A. Similar effects are observed for Chalc1 (Fig. 7B) and data for both probes are reported in Table 1. A blue shift and an increase of the intensity are observed. We interpret these changes by the fact that the anionic form of the boron group acts as an electron donating group to the carbonyl group. This increase of the electronic density on the carbonyl decreases the importance of the ICT and then induces the spectral changes observed. The spectral shifts for both chalcone derivatives (~15 nm) are much smaller than the previous probes described above. On the other hand, the intensity change is larger in comparison with the stilbene and diphenylbutadiene derivatives. The chalcone derivatives have also the advantage of displaying a longer wavelength of absorption and emission, but have a small fluorescence quantum yield.

Figure 7B shows the titration of both chalcone derivatives against fluoride. As observed for the other derivatives, no effect of chloride and bromide has been observed on the spectral properties of these derivatives. The stability constants of both chalcones (Table 1) are 10- to 20-fold larger than the other derivatives. The stability constants of Chalc1 (1.2×10^4 dm^9 mol^{-3}) and Chalc2 (1.5×10^4 dm^9 mol^{-1}) are very similar in comparison with stability constants observed for the phenylboronic acid (1.04×10^4 dm^9 mol^{-1}) and anthrylboronic acid (1.08×10^4 dm^9 mol^{-1}) derivatives (25). This could indicate that the boronic acid group in the chalcone derivative is less involved in the ICT than the other derivatives presented in this study.

DISCUSSION

Fluorescent probes are known to be very useful for many applications. Their uses have led to important developments in fluorescence microscopy, DNA technology, and fluorescence sensing. To be useful, the probes should show different spectral properties; in addition, the chelator group and the mechanism should be easy to adapt to different fluorophores. This is important to give flexibility for the different applications where these probes could be useful. The boronic acid group has shown to be selective against fluoride. Since the boronic acid group also interacts with the hydroxyl ion and diols (9), fluorescence sensing of fluoride could be compromised at high pH and in the presence of some diols (particularly catechols and sugars). Numerous boronic acid compounds are available commercially, particularly numerous reactive substituted phenylboronic acids are available and can be easily coupled to make desirable probes. In this study, we have shown that the use of the ICT, involving the boronic acid group, has lead to interesting spectral changes in the presence of fluoride and can be applied to different fluorophores. The use of the ICT mechanism has lead to wavelength-ratiometric probes and/or probes showing an increase of fluorescence intensity in the presence of fluoride. In addition, we showed that the ICT mechanism is useful for

developing fluorescence probes for fluoride showing emission throughout the visible wavelength.

ACKNOWLEDGMENTS

REFERENCES

1. de Silva AP, Fox DB, Moody TS, and Weir SM (2001) Trends Biotechnol. 19, 29–34. [PubMed: 11146100]

2. de Silva AP, Fox DB, Huxley AJM, and Moody TS (2000) Coord. Chem. Rev 205, 41–57.

3. Valeur B, and Leray I (2000) Coord. Chem. Rev 205, 3–40.

4. Huston ME, Akkaya EU, and Czarnik AW (1989) J. Am. Chem. Soc 111, 8735–8737.

5. Haugland RP (1996) Handbook of Fluorescent Probes and Research Chemicals, Chaps. 22, 23, and 24. Molecular Probes, Inc., Eugene, OR.

6. Burtis CA, and Ashwood ER (1999) Tietz Textbook of Clinical Chemistry, third Ed., Saunders, Philadelphia.

7. Valeur B (1994) Topics in Fluorescence Spectroscopy (Lakowicz JR, Ed.), pp. 21–50, Plenum, New York.

8. Rettig W, and Lapouyade R (1994) Topics in Fluorescence Spectroscopy (Lakowicz JR, Ed.), pp. 109–150, Plenum, New York.

9. Lorand JP, and Edwards JO (1959) J. Org. Chem 24, 769–774.

10. Katz HE (1986) J. Am. Chem. Soc 108, 7640–7645. [PubMed: 22283269]

11. Hartley JH, James TD, and Ward CJ (2000) Perkin Trans. I 19, 3155–3184.

12. James TD, Samankumara Sandanayake KRA, and Shinkai S (1996) Angew. Chem. Int. Ed. Engl 35, 1910–1922.

13. Tong A-J, Yamauchi A, Hayashita T, Zhang Z-Y, Smith BD, and Teramae N (2001) Anal. Chem 73, 1530–1536. [PubMed: 11321305]

14. Yang W, He H, and Drueckhammer DG (2001) Angew. Chem. Int. Ed 40, 1714–1718.

15. DiCesare N, and Lakowicz JR (2001) J. Phys. Chem. A, 105, 6834–6840. [PubMed: 31427854]

16. DiCesare N, and Lakowicz JR (2001) J. Photochem. Photobiol. A 143, 39–47.

17. (a)Di Cesare N, and Lakowicz JR (2001) Chem. Commun 19, 2022–2023;(b)Di Cesare N, and Lakowicz JR (2001) Chem. Phys. Lett, submitted.

18. Rum G, Lee W-Y, and Gardea-Torresdey J (2000) J. Chem Edu 77, 1604–1606.

19. Ekstrand J (1996) Fluoride metabolism in Fluoride in Dentistry, 2nd Ed. (Fejerskov O, Ekstrand J, and Burt BA, Eds.), p. 55, Munksgaard, Copenhagen.

20. Frant MS, and Ross JW (1966) Science 154, 1553–1555. [PubMed: 5924922]

21. Dusemund C, Samankumara Sandanayake KRA, and Shinkai S (1995) Chem. Commun 3, 333–334.

22. Nicolas M, Fabre B, Chapuzet JM, Lessard J, and Simonet J (2000) J. Electroanal. Chem 482, 211–216.

23. Yamamoto H, Ori A, Ueda K, Dusemund C, and Shinkai S (1996) Chem. Commun 3, 407–408.

24. Ward CJ, Patel P, and James TD (2001) Chem. Lett 5, 406–407.

25. Cooper CR, Spencer N, and James TD (1998) Chem. Commun 13, 1365–1366.

26. Valeur B, Pouget J, Bourson J, Kaschke M, and Emsting P (1992) J. Phys. Chem 96, 6545–6549.

27. Diwu Z, Lu Y, Zhang C, Klaubert DH, and Haugland RP (1997) Photochem. Photobiol 66, 424–431.
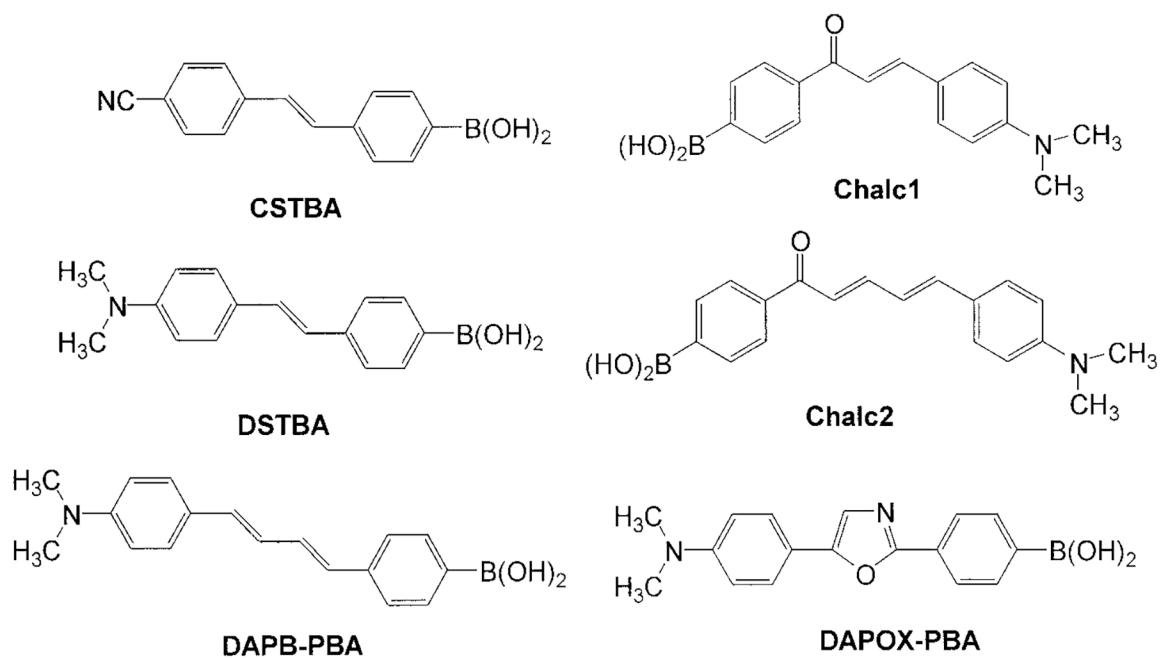
FIG. 1.
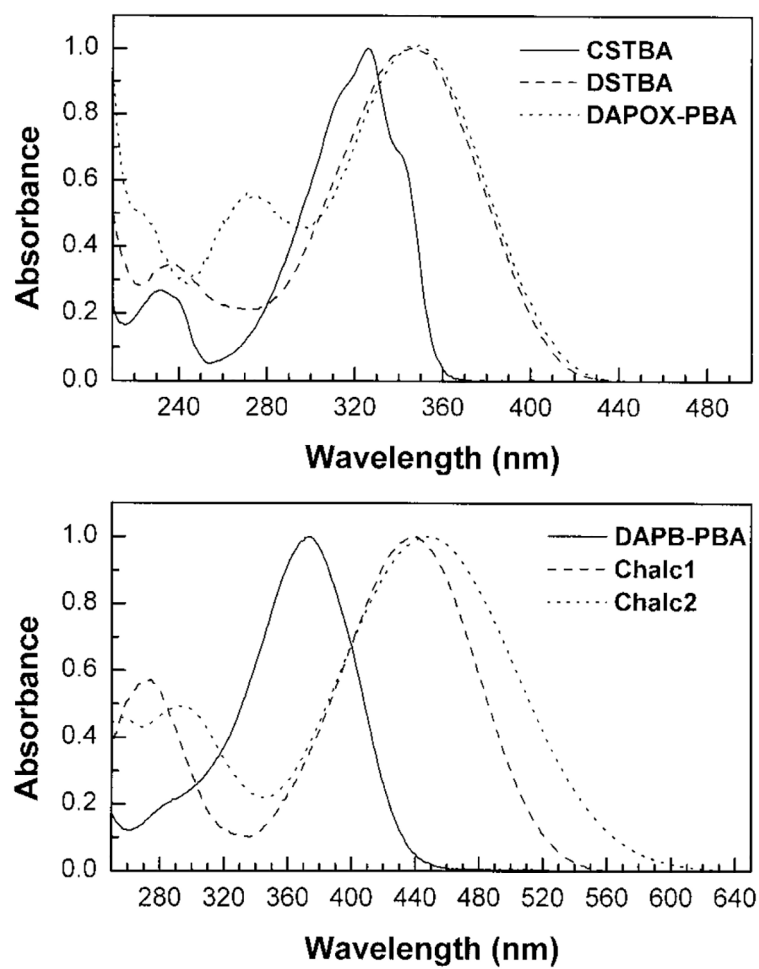Molecular structure of the investigated probes.

FIG. 2.
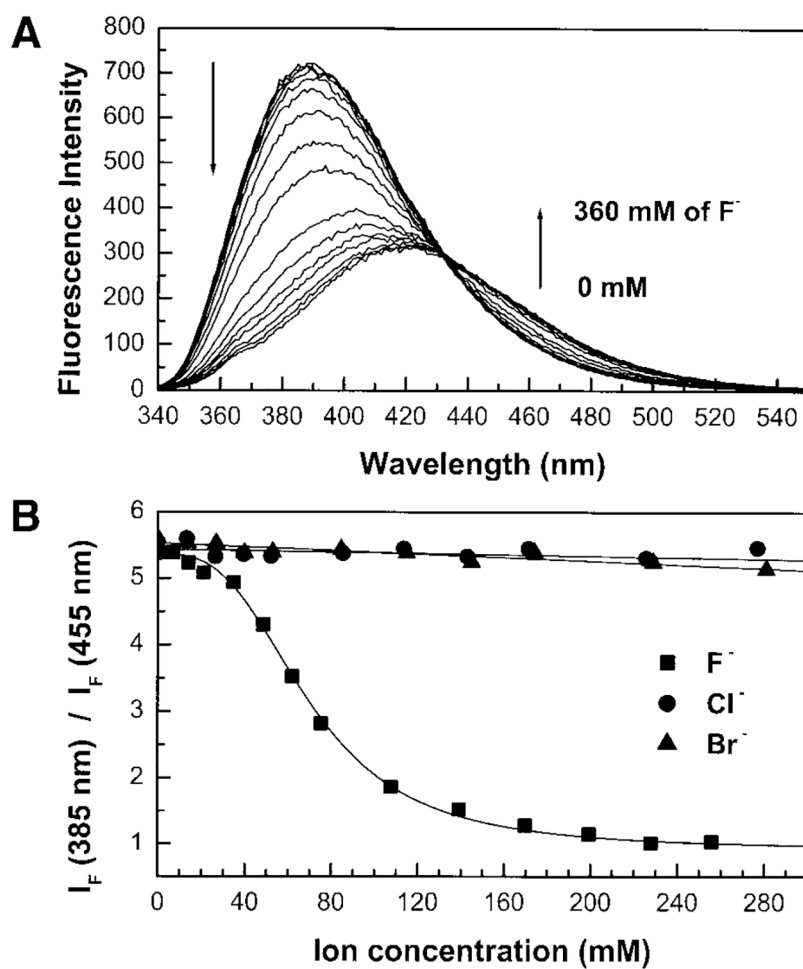Absorption spectra of the investigated probes, measured in water/methanol (2:1 v/v) at room temperature.

FIG. 3.
(A) Emission spectrum of CSTBA in the presence of fluoride, measured in water/methanol (2:1 v/v) at room temperature, $\lambda_{ex} = 325$ nm. (B) Titration curves against fluoride, chloride, and bromide.
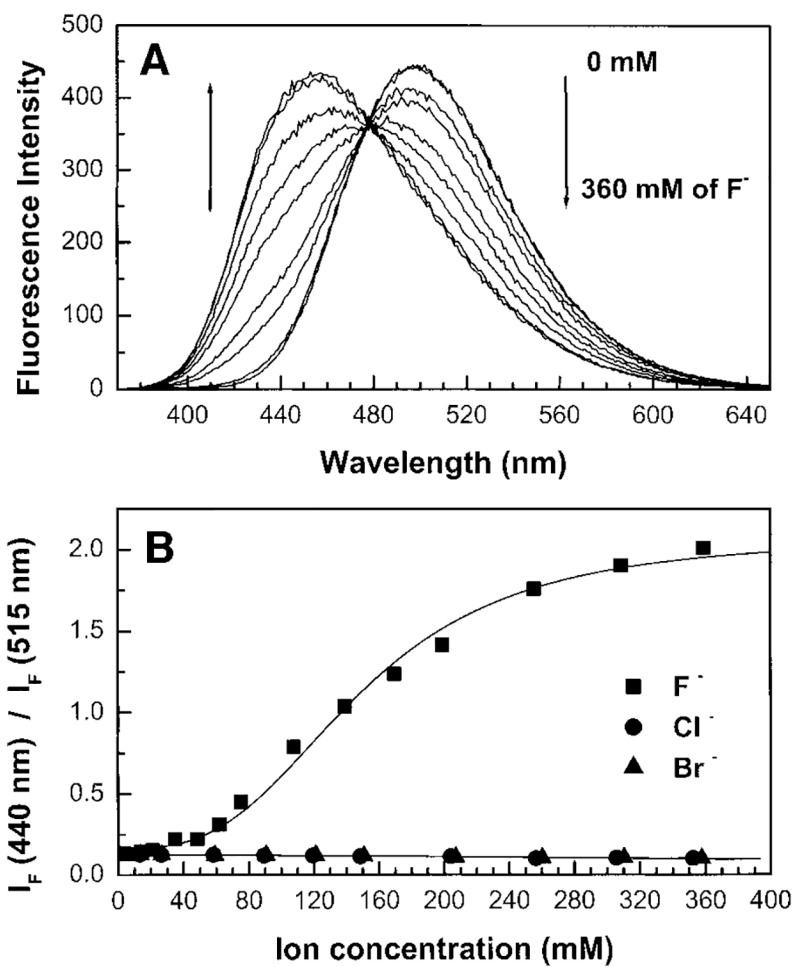
FIG. 4.
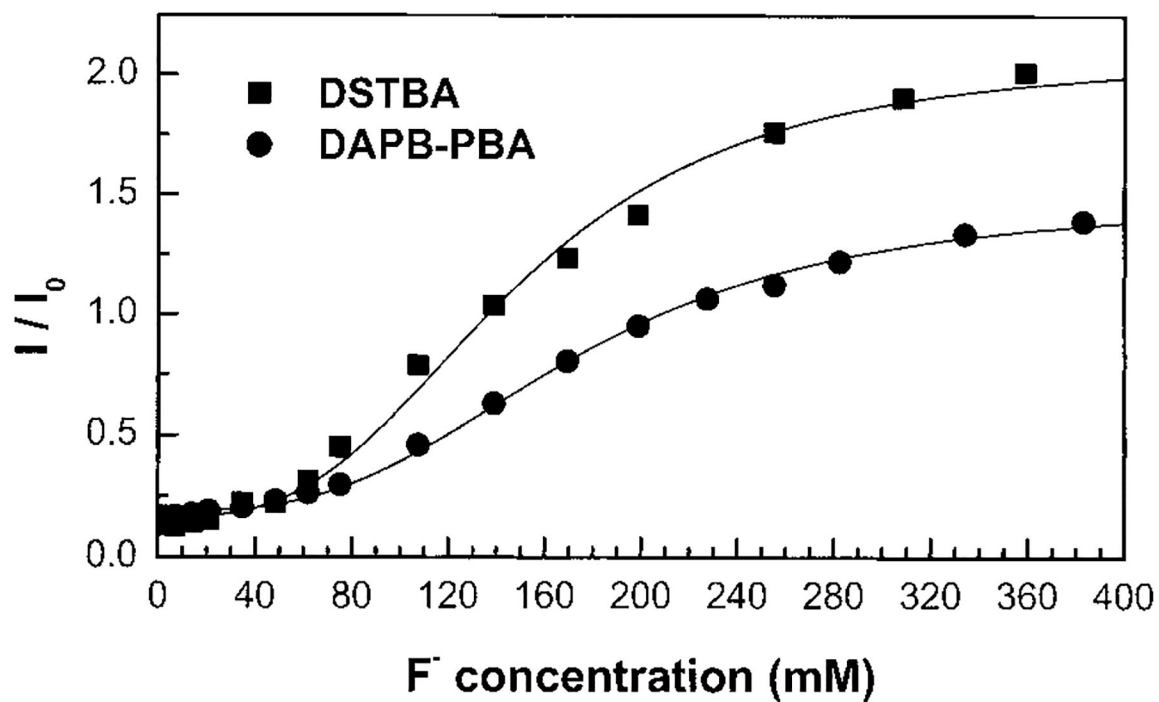(A) Fluoride effect on the emission spectrum of DSTBA, measured in water/methanol (2:1 v/v) at room temperature, λ_{ex} = 345 nm. (B) Titration curves against fluoride, chloride, and bromide.

FIG. 5.
Titration curves against fluoride for DSTBA and DAPB-PBA, measured in water/methanol (2:1 v/v) at room temperature. I_A and I_B values are 440/515 and 465/550 nm for DSTBA and DAPB-PBA, respectively.
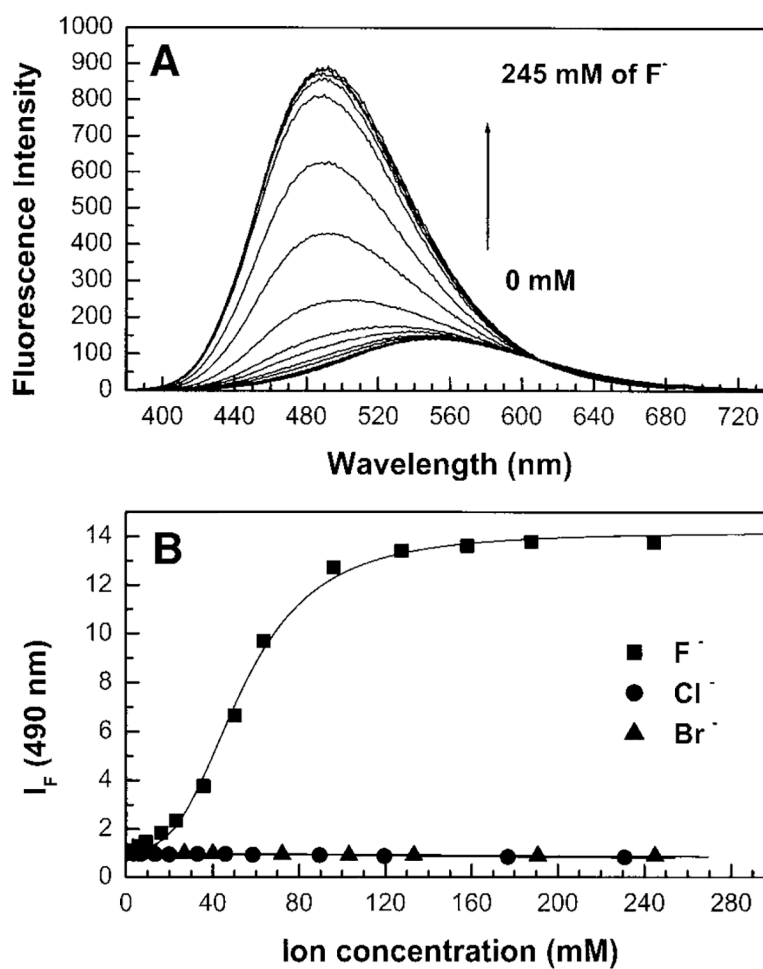
FIG. 6.
(A) Emission spectrum of DAPOX-PBA in the presence of fluoride, measured in water/methanol (2:1 v/v) at room temperature, $\lambda_{ex} = 345$ nm. (B) Titration curves against fluoride, chloride, and bromide.
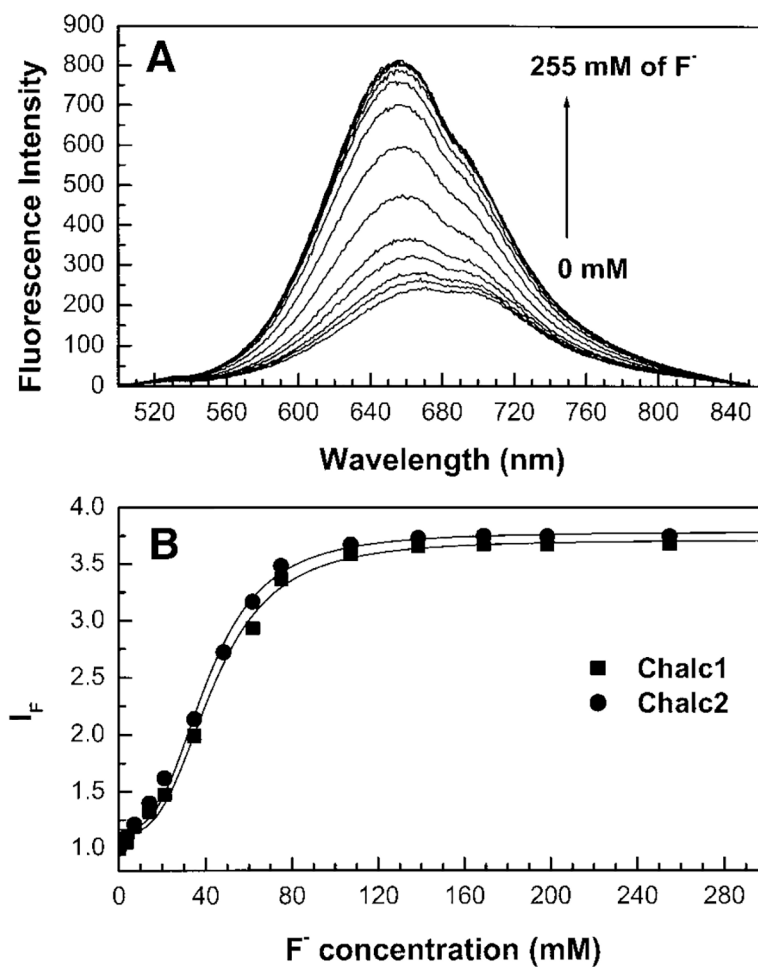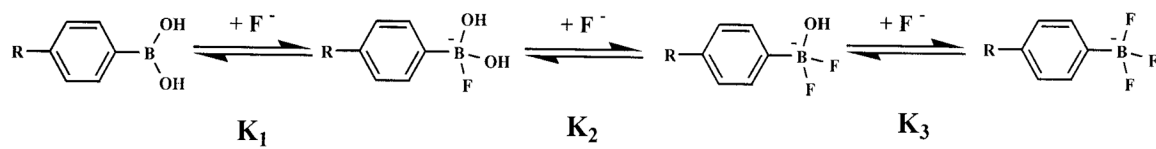
FIG. 7.
(A) Emission spectrum of Chalc2 in the presence of fluoride, measured in water/methanol (2:1 v/v) at room temperature, λ_{ex}= 450 nm. (B) Titration curves against fluoride, for Chalc1 and Chalc2. I_F values are 565 and 650 nm for the two compounds, respectively.

SCHEME 1.

Equilibrium involved in the interaction between the boronic acid group and fluoride.

TABLE 1

Spectroscopic Parameters and Stability Constants of the Investigated Probes in the Absence and in the Presence of Fluoride Measured in Water/Methanol 2:1 (v/v)

Probe	λ_{abs} (nm)	ϵ (M^{-1} cm^{-1})	λ_F (ϕ_F) (nm)	λ_F (with F$^-$) (nm)	I/I_0	K_3 (dm^9 mol^{-3})
CSTBA	326	47300	389 (0.006)[a]	420	0.44	2.9×10^3
DSTBA	347	28900	497 (0.088)[a]	455	0.96	3.0×10^2
DAPOX-PBA	347	20400	554 (0.17)[b]	490	14	6.6×10^3
DAPB-PBA	373	—	531	488	0.67	1.9×10^2
Chalc1	438	21800	585 (0.006)[b]	570	3.7	1.2×10^4
Chalc2	449	19000	668 (0.007)[b]	654	3.8	1.5×10^4

[a]Taken from (15).

[b]Taken from (17).